Direct Electrodeposition of ZnO Nanotube Arrays in Anodic Alumina Membranes

Liang Li,* Shusheng Pan, Xincun Dou, Yonggang Zhu, Xiaohu Huang, Youwen Yang, Guanghai Li, and Lide Zhang

Anhui Key Laboratory of Nanomaterials and Nanotechnology, Institute of Solid State Physics, Chinese Academy of Sciences, P. O. Box 1129, Hefei 230031, People's Republic of China

Received: February 9, 2007; In Final Form: March 24, 2007

Semiconductor ZnO nanotube arrays have been synthesized by direct electrochemical deposition from aqueous solutions into porous anodic alumina membranes. Scanning electron microscopy and transmission electron microscopy indicate that large-area and highly ordered nanotube arrays have been obtained. X-ray diffraction and selected-area electron diffraction analyses show that the as-synthesized nanotubes are polycrystalline. Photoluminescence spectra of the ZnO nanotube arrays show that a violet peak and a blue peak are centered at 414 and 464 nm, respectively. The ordered polycrystalline ZnO nanotube arrays may find potential applications in optoelectronic and sensor devices. The growth mechanism and the electrochemical deposition process are discussed.

Introduction

Zinc oxide (ZnO), a wide band gap (3.37 eV) semiconductor with high exciton binding energy (60 meV), has a wide range of applications in sensors, optoelectronic devices, and photonic detectors.[1] Recently, a variety of techniques have been developed to fabricate one-dimensional (1D) ZnO nanostructures, including nanowires, nanorods, and nanobelts, such as metal−organic chemical vapor deposition, infrared irradiation, thermal evaporation through vapor−liquid−solid, vapor−solid mechanisms, and template technology.[2−4] In contrast, few publications on the preparation of ZnO nanotubes have been reported because the tubular form is generally available in layered materials such as carbon nanotubes, so it seems difficult to obtain the tubular structure for the unlayered ZnO materials. ZnO nanotubes have only been fabricated by vapor-phase deposition, thermal oxidation, a sol−gel process, and a hydrothermal process.[5,6]

It is well-known that the special hollow structure provides ZnO with more prominent advantages than other 1D ZnO materials; for example, the enhanced confinement effect in 1D hollow structures tune electronic properties in a wider range, and a larger area−volume ratio provides an effective way to optimize the performances of devices in catalysts, gas sensors, and solar cells. Especially the polycrystalline ZnO nanotubes with the tube walls composed of nanoparticles, which have a larger specific surface area than single-crystalline tube structures, are expected to be useful as photocatalysts and sensors with improved performances.[7]

Templated synthesis has been employed widely to prepare nanowires and nanorods of defined dimension. Several techniques of forming nanomaterials in templates have been developed such as chemical vapor deposition (CVD), sol−gel deposition, polymerization, and electrochemical deposition, in which electrodeposition has emerged as a favored method for the formation of conducting nanomaterials (metals, semiconductors, and polymers).[8−11] As we know, generally a sol−gel process is necessary for obtaining metal oxide nanowires and nanotubes in templates, and post-thermal treatment must be carried out to make samples crystallizable. In recent publications, our group and other researchers have demonstrated how metal nanotubes can be prepared in the nanochannels of a porous anodic alumina membrane (AAM) using an electrochemical deposition technique.[12] Here we illustrate how this approach can be employed to deposit ZnO nanotube arrays in AAM, and their photoluminescence property was investigated. To our knowledge this is the first time that the formation of ZnO nanotubes by direct electrodeposition in AAM has been reported.

Experimental Section

The AAM was prepared using a two-step anodization process as described previously.[13] Direct electrodeposition of ZnO nanotubes was performed in an AAM of thickness 25 μm, pore diameter 80 nm, and pore density of 1.0×10^{11} pores/cm^2. A layer of gold film was evaporated onto one surface of the membrane to serve as the working electrode in a common two-electrode plating cell, and a graphite plate was used as the counter electrode. The electrolyte was prepared by dissolving 0.01 M $Zn(NO_3)_2 \cdot 6H_2O$ in deionized water. Material was deposited in the templates using potentials ranging between 1.5 and 1.8 V with deposition times ranging from 60 to 150 min at 85 °C.

Power X-ray diffraction (XRD; Philips PW 1700x with Cu Kα radiation), field-emission scanning electron microscopy (FE-SEM; FEI Sirion-200), and high-resolution transmission electron microscopy (HRTEM; JEM-2010) with selected-area electron diffraction (SAED) analyses were used to study crystalline structures and morphologies of nanotube arrays. The chemical composition of the nanotubes was determined by an energy-dispersive spectrometer (EDS). Photoluminescence (PL) spectra were carried out by Edinburgh FLS920 fluorimeter instruments with the excitation wavelength 333 nm at room temperature. For XRD measurements, the overfilled nanotubes on the surface of the AAM were mechanically polished using Al_2O_3 nanopowder. For SEM imaging and PL collection, the AAM was partly dissolved with 0.5 M NaOH solution, and then carefully rinsed three times with deionized water. For HRTEM observations,

* Corresponding author. Fax: +86-551-5591434. E-mail: liliang@issp.ac.cn.

10.1021/jp0711242 CCC: $37.00 © 2007 American Chemical Society
Published on Web 04/28/2007

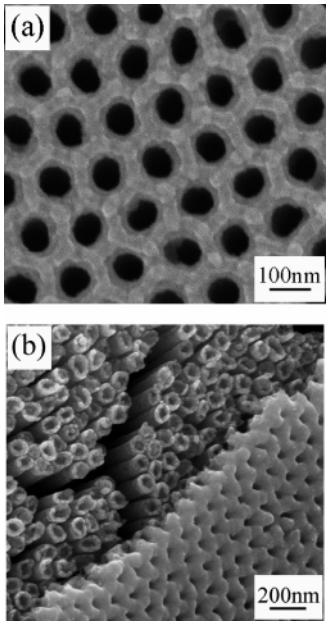

Figure 1. SEM image of the bottom surface of (a) empty AAM with a sputtered Au layer and (b) AAM after electrodepositing ZnO nanotubes.

the AAM was completely dissolved with 1 M NaOH solution and then rinsed with absolute ethanol.

Results and Discussion

Figure 1a shows the SEM image of empty AAM with a sputtered Au film on the bottom surface. It can bee seen that thin Au film was sputtered mainly on the top part of the inner pore surface to form rings and covers only a few parts of the pore of the AAM. After the electrodeposition of ZnO nanotubes (the top-left corner of Figure 1b), the nanopores of AAM become narrow due to the fact that the ZnO species grow initially in the sites at which Au clusters locate, as shown in the bottom-right corner of Figure 1b.

Figure 2a−c shows the top-surface and cross-sectional SEM images of ZnO nanotubes after etching AAM for different times. Apparently, the nanotubes replicate the pore morphology of AAM and are of large area and highly ordered. The cross-sectional images indicate that all the ZnO nanotubes have almost the same length (about 25 μm), which is the same as the thickness of the AAM used, because the deposition of ZnO nanotubes starts at the Au cathode on the bottom of the nanochannels and then grows along the channels until the top of the AAM, at the same time, implying that the ZnO particles grow along the pores at the same rate. The enlarged image of the top surface of ZnO nanotubes (Figure 2d) clearly shows that the tube walls are composed of nanoparticles.

XRD measurement was performed to probe the crystal structure and phase purity of the ZnO nanotubes. Figure 3a shows a typical XRD pattern of the ZnO nanotubes embedded in AAM. All the diffraction peaks can be indexed to a hexagonal wurtzite structured ZnO phase (JCPDS File 80-0075). The EDSs (Figure 3b) further confirm that the nanotubes are composed of zinc and oxygen with an atomic ratio of about 1:1.

The morphology and structure of an individual ZnO nanotube have been characterized in further detail using HRTEM and SAED, as shown in Figure 4. The HRTEM image suggests that the end of the nanostructure is hollow, and the tube wall is composed of nanoparticles. It can be seen that the nanotube is straight and uniform along its whole length. However, the wall

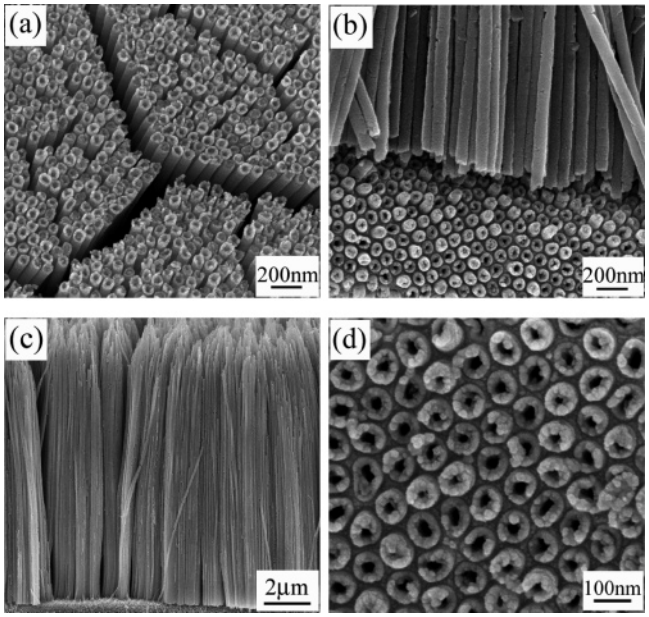

Figure 2. SEM images of ZnO nanotube arrays after etching AAM for different times: (a) top surface, 3 min; (b, c) cross section, 5 and 8 min; (d) magnified image of selected area in (a).

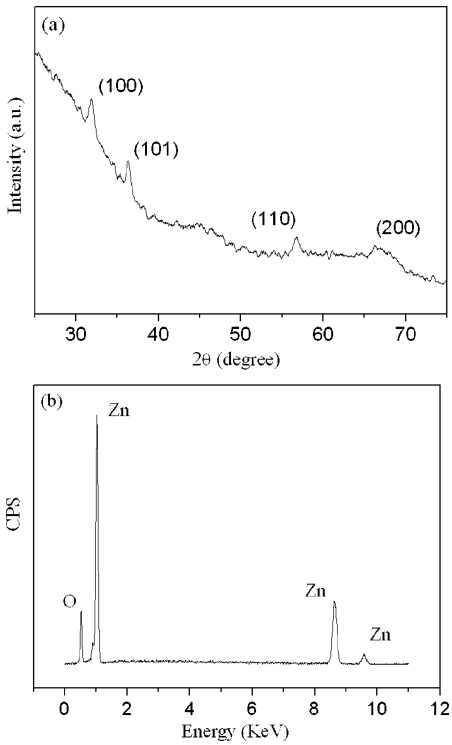

Figure 3. XRD pattern (a) and EDS spectrum (b) of ZnO nanotubes.

thickness is very large, so it is very difficult to obain the hollow contrast image of the tube surface and the lattice fringes. The corresponding SAED pattern shows that the ZnO nanotubes are polycrystalline and the diffraction pattern can be indexed as the (101), (110), and (112) lattice planes of hexagonal wurtzite ZnO.

A schematic of the growth mechanism for the ZnO nanotubes is shown in Figure 5. To synthesize ZnO nanotube arrays, the thickness of the Au layer sputtered on the bottom surface of AAM should be thin enough to not completely cover the pores of AAM.

As we know, for sol−gel based preparation of ZnO nanomaterials in AAM, it is generally accepted that OH^- ions

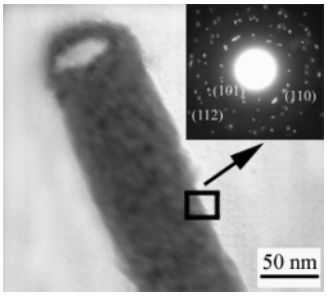

Figure 4. HRTEM image of the ZnO nanotubes with the corresponding SAED pattern inserted in the top-right corner.

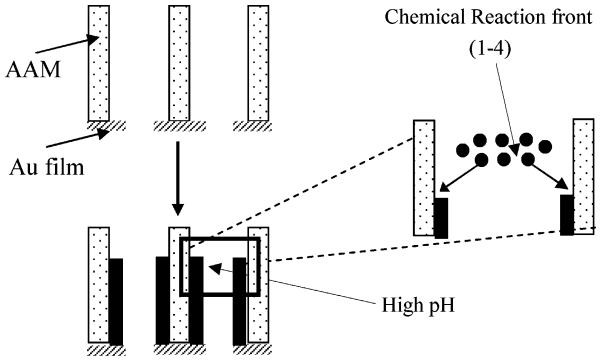

Figure 5. Schematic of fabrication of ZnO nanotubes by direct electrodeposition.

released from hydrolysis react with Zn^{2+} ions to form $Zn[(OH)_x]$-$(H_2O)_y$ sol, which could be transformed into crystalline ZnO via a post-high-temperature-annealing process. Here, from the viewpoint of chemical reactions, the direct electrochemical deposition reactions to prepare ZnO nanotubes are proposed as follows:

$$Zn(NO_3)_2 \rightarrow Zn^{2+} + 2NO_3^- \quad (1)$$

$$NO_3^- + H_2O + 2e^- \rightarrow NO_2^- + 2OH^- \quad (2)$$

$$Zn^{2+} + 2OH^- \rightarrow Zn(OH)_2 \quad (3)$$

$$Zn(OH)_2 \rightarrow ZnO + H_2O \quad (4)$$

Reduction of the nitrate (NO_3^- to NO_2^-) in mild acid solution of Zn^{2+}, which results in an increase of the pH near the Au electrode surface, is crucial.[14] With increasing concentration of OH^-, $Zn(OH)_2$ will form and deposit on the cathode electrode. The deposited $Zn(OH)_2$ will subsequently be decomposed and form ZnO at a temperature of 85 °C. The depletion of Zn^{2+} within the nanopores and the continual production of OH^- at the Au electrode surface lead to a chemical reaction front that propagates along the nanopores. As the reaction proceeds, ZnO particles are further produced along the tubes; thus the length of the nanotubes continually increase with the deposition time.

Figure 6 shows the PL spectrum of the ZnO nanotubes embedded in partly removed AAM at room temperature. The emitting band centered at 420 nm has been observed. This asymmetric band can be well fitted by two Gaussian structures at 414 and 464 nm. Recently, violet and blue luminescence such as 413, 420, 465, and 480 nm from ZnO thin films, nanoparticles, and other nanostructures have been reported.[15] Violet emissions at 413 nm have been attributed to the possible

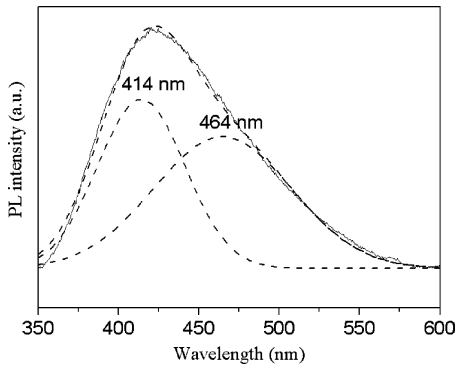

Figure 6. Room-temperature PL spectrum of ZnO nanotubes under excitation at 333 nm.

existence of cubic ZnO.[16] However, in the present nanostructures the emission centered at 414 nm did not originate from cubic ZnO due to the pure hexagonal wurtzite phase of ZnO nanotubes (see Figure 3a). It can possibly be due to the interstitial oxygen or transition between defects (interface traps) at grain boundaries and the valence band.[15] The blue band at 464 nm may originate from the defect structures, which was also previously observed for ZnO nanotubes and nanorods.[5,17] It is also noticed that the UV peak (usually observed in ZnO crystals) did not appear here, which is due to the polycrystalline structure of the ZnO nanotubes.

Conclusions

It has been demonstrated that the electrodeposition of ZnO within a porous AAM with a sputtered Au electrode yields polycrystalline ZnO nanotubes. In all the previous reports, formation of ZnO nanotubes in templates has involved sol−gel processes, in which a sol of the ZnO is formed in the template and then thermally treated to become crystalline. The electrodeposition approach to nanotubes offers the obvious advantage that the deposition of particles starts at the Au cathode on the bottom of the nanopores and the length of ZnO nanotubes can be easily controlled by the deposition time, and that the formed nanotubes are crystals with no any post-thermal treatment. We believe that this technology offers a new and convenient route to fabricate metal oxide nanotube arrays and may find potential application in optoelectronic and sensing devices and so on.

Acknowledgment. This work was supported by the National Natural Science Foundation of China (No. 10674137), National Major Project of Fundamental Research for Nanomaterials and Nanostructures (No. 2005CB623603), Special Project of Excellent Young Researchers of Anhui Province, and Support Project of Excellent President Scholarship of Chinese Academy of Sciences.

References and Notes

(1) Law, M.; et al. *Annu. Rev. Mater. Res.* **2004**, *34*, 83. Kong, X. Y.; et al. *Appl. Phys. Lett.* **2004**, *84*, 975.

(2) Fang, X. S.; et al. *J. Mater. Sci., Technol.* **2006**, *22*, 1. Fang, X. S.; et al. *Chem. Lett.* **2005**, *34*, 436. Zhang, X. H.; et al. *Appl. Phys. Lett.* **2007**, *90*, 013107. Xu, L. F.; et al. *J. Phys. Chem. B* **2005**, *109*, 13519.

(3) Wang, Z. *Langmuir* **2004**, *20*, 3441. Lao, J. Y.; et al. *J. Mater. Chem.* **2004**, *14*, 770. Geng, B. Y.; et al. *Appl. Phys. Lett.* **2003**, *82*, 4791. Ye, C. H.; et al. *J. Phys. Chem. B* **2005**, *109*, 19758. Wan Q.; et al. *Appl. Phys. Lett.* **2004**, *84*, 3654. Cheng, B. *Chem. Commun.* **2004**, 986.

(4) Wu, X. F.; et al. *Chem. Commun.* **2006**, 1655. Gao, P. X.; et al. *Small* **2005**, *1*, 945. Yang, J. L.; et al. *Adv. Mater.* **2004**, *16*, 1661. Hosono, E.; et al. *Adv. Mater.* **2005**, *17*, 2091. Li, P.; et al. *Chem. Commun.* **2004**, *24*, 2856. Lai, M. *Chem. Mater.* **2006**, *18*, 2233.

(5) Jeong, J. S.; et al. *Chem. Mater.* **2005**, *17*, 2752. Zhang, X. H.; et al. *J. Phys. Chem. B* **2003**, *107*, 10114. Wu, G. S.; et al. *Solid State Commun.* **2005**, *134*, 485. Vayssieres, L.; et al. *Chem. Mater.* **2001**, *13*, 4395. Shen, X. P.; et al. *Nanotechnology* **2005**, *16*, 2039.

(6) Chen, S. J.; et al. *Appl. Phys. Lett.* **2006**, *88*, 133127. Sun, Y.; et al. *Adv. Mater.* **2005**, *17*, 2477. Tong, Y. H.; et al. *J. Phys. Chem. B* **2006**, *110*, 14714. Xu, W. Z.; et al. *Appl. Phys. Lett.* **2005**, *87*, 093110.

(7) Li, Q. H.; et al. *Appl. Phys. Lett.* **2005**, *86*, 123117. Wan, Q.; et al. *Appl. Phys. Lett.* **2004**, *84*, 124. Rout, C. S.; et al. *Chem. Phys. Lett.* **2006**, *418*, 586.

(8) Xu, D. S.; et al. *J. Phys. Chem. B* **2000**, *104*, 5061. Choi, J.; et al. *Chem. Mater.* **2003**, *15*, 776. Li, T.; et al. *Nanotechnology* **2005**, *15*, 1479. Zhao, J. L.; et al. *Nanotechnology* **2005**, *16*, 2450. Lai, M. *J. Mater. Chem.* **2006**, *16*, 2843.

(9) Lakshmi, B. B.; et al. *Chem. Mater.* **1997**, *9*, 2544. Guo, Y. G.; et al. *J. Phys. Chem. B* **2003**, *107*, 5441. Li, C. J.; et al. *Adv. Mater.* **2005**, *17*, 71.

(10) Yanagishita, T.; et al. *Adv. Mater.* **2004**, *16*, 429. Lee, W.; et al. *Angew. Chem., Int. Ed.* **2005**, *44*, 6050.

(11) Han, G. C.; et al. *J. Appl. Phys.* **2003**, *93*, 9202. Xu, Q.; et al. *J. Phys. Chem. B* **2003**, *107*, 8294. Cao, H.; et al. *Adv. Mater.* **2001**, *13*, 121.

(12) Li, L.; et al. *Appl. Phys. Lett.* **2006**, *88*, 103119. Lee, W.; et al. *Chem. Mater.* **2005**, *17*, 3325. Davis, D. M.; et al. *Electrochem. Solid State Lett.* **2005**, *8*, D1.

(13) Li, L.; et al. *Small* **2006**, *2*, 548. Li, L.; et al. *J. Phys. Chem. B* **2004**, *108*, 19380.

(14) Peulon, S.; et al. *Adv. Mater.* **1996**, *8*, 166. Izaki, M. *Appl. Phys. Lett.* **1996**, *68*, 2439.

(15) Xu, X. L.; et al. *J. Cryst. Growth* **2001**, *223*, 201. Jin, B. J.; et al. *Thin Solid Films* **2000**, *366*, 107. Hu, J. Q.; et al. *Chem. Phys. Lett.* **2001**, *344*, 97. Dai, L.; et al. *J. Phys.: Condens. Matter* **2003**, *15*, 2221.

(16) Sekiguchi, T.; et al. *J. Cryst. Growth* **2000**, *214/215*, 68.

(17) Wu, J. J.; et al. *Adv. Mater.* **2002**, *14*, 215.